available at www.sciencedirect.com

ScienceDirect

journal homepage: www.elsevier.com/locate/agrformet

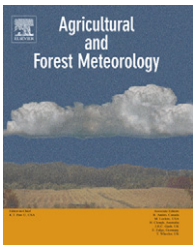

Extrapolating gross primary productivity from leaf to canopy scale in a winter wheat crop

Julien Hoyaux [a,*], *Christine Moureaux* [a], *Denis Tourneur* [b], *Bernard Bodson* [b], *Marc Aubinet* [a]

[a] *Unité de Physique des Biosystèmes, Faculté Universitaire des Sciences Agronomiques de Gembloux, 8 Avenue de la Faculté, B-5030 Gembloux, Belgium*

[b] *Unité de Phytotechnie des Régions tempérées, Faculté Universitaire des Sciences Agronomiques de Gembloux, 2 Passage des Déportés, B-5030 Gembloux, Belgium*

ARTICLE INFO

Article history:
Received 22 May 2007
Received in revised form
16 November 2007
Accepted 23 November 2007

Keywords:
Winter wheat
Photosynthesis
Scaling up
Gross primary productivity
Carboeurope

ABSTRACT

The objectives of this paper are to determine winter wheat gross primary productivity (GPP) by extrapolating to the canopy scale measurements of photosynthetic assimilation made at the leaf scale, to identify the uncertainties inherent in this method and to quantify their impact on GPP predictions. Crop development monitoring and photosynthesis measurements were conducted between 1 May and 19 July 2004 at the Carboeurope site of Lonzée, Belgium, with a portable porometer Li-Cor 6400. The model divided the canopy into 10 layers in which assimilation was computed on the basis of incident radiation and of assimilation to light response curves calibrated in the field. The model also took account of photosynthesis of stems and ears, senescent organ distribution and response of assimilation to leaf to air vapour pressure difference. Model estimates were compared with eddy covariance measurements performed at the site during the same period. The best agreement (regression slope = 1.13, R^2 = 0.94) between the two estimates was obtained by postulating a concentration of the senescent organs in the canopy bottom and a stem assimilation rate equal to 63% of the leaf assimilation. This ratio was found compatible with further leaf scale measurements. This led to a GPP of 1570 g C m^{-2} during the crop development and maturation periods. The sensitivity analysis revealed that the main sources of uncertainties were linked to the photosynthetic capacity of the stems (an increase of 40% in the initial GPP) and ears (an additional increase of 15%) and to the senescent organ spatial distribution (impact of 7–9%). An overestimation of GPP during spring (270 g C m^{-2}) was also observed, due to assimilation reduction at low temperature not be accounted for. Apart from this, the impact of the A–Q curve parameter uncertainties was found to be limited (impact on GPP always lower than 4%).

© 2007 Elsevier B.V. All rights reserved.

* *Corresponding author*. Tel.: +32 81 62 24 88; fax: +32 81 62 24 39.
E-mail address: hoyaux.j@fsagx.ac.be (J. Hoyaux).

Abbreviations: α, quantum yield; A, net assimilation; A_s, net assimilation at saturating light; D_s, air saturation deficit; D_l, leaf to air vapour pressure difference; EAI, ear area index; GLAI, green leaf area index; GPP, gross primary productivity; G_s, gross assimilation at saturating light; PPFD, photosynthetic photon flux density; PsAI, photosynthetic area index; Q, photosynthetic photon flux density; R_d, dark respiration; SAI, stem area index; T_a, air temperature; T_l, leaf temperature; VAI, total vegetation area index; YLAI, yellow leaf area index.

0168-1923/$ – see front matter © 2007 Elsevier B.V. All rights reserved.
doi:10.1016/j.agrformet.2007.11.010

1. Introduction

Croplands occupy about one-third of the land surface in Europe (FAO Statistical Databases, 2003) and 45% of the land surface in Belgium (MRW-DGA, 2005). They have the potential to mitigate about 16–19 Tg C y^{-1} (Freibauer et al., 2004). Their impact on the terrestrial carbon cycle is therefore significant and this justifies the recent development of CO_2 flux measurements at these sites (e.g., Soegaard and Thorgeirsson, 1998; Anthoni et al., 2004; Suyker et al., 2004). The present study is part of a larger research project whose overall goal is to establish the carbon balance of an agricultural site under a 4-year rotation system, which is typical of the Hesbaye region (Moureaux et al., 2006).

The goal of this research is to evaluate the feasibility of scaling up the assimilation measurements from leaf to crop scale. Scaled-up leaf measurements might provide useful information for validating eddy covariance measurements or refining the description of the various flux contributions to the net ecosystem exchange. The combination of these measurements for establishing the crop carbon balance is described in another paper (Moureaux et al., in press).

In this paper, we concentrate on the scaling up procedure. An extrapolation scheme was developed based on assimilation to radiation responses (A–Q curves) obtained by porometry measurements performed at the leaf scale during the study and on an evaluation of light absorption by the crop. Continuous micrometeorological measurements performed at the site meteorological station were used as input data, as well as the vegetation element distribution in the crop that was continuously monitored throughout season. The scaled-up results were compared with eddy covariance flux estimations and the differences were discussed. In addition, an uncertainty analysis was developed in order to determine the most important causes of uncertainties that affected the scaled-up GPP. This analysis allowed us to identify the most critical parameters to prioritize during field measurements and scaling up procedures. Although the approach was developed on a specific site and in a specific season, we consider that most of the results presented here could be extrapolated to cereal crops.

2. Material and methods

2.1. Site description

The site is a crop field in Lonzée, near Gembloux in Belgium (50°33′N, 4°44′E). It is described in detail by Moureaux et al. (2006). The climate is typically oceanic temperate. From 1 October to 25 Augustus the overall precipitation and average air temperature at the site were 545 mm and 10 °C, respectively. The soil is a luvisol and the site is flat, with a mean gradient of less than 1.2%. The site is included in the Carboeurope IP, Fluxnet and IMECC networks.

The site was equipped with an eddy covariance system and a meteorological station. The eddy covariance system measured fluxes of CO_2, water vapour and sensible heat. It was placed at a height of 2.7 m and consisted of a research-grade sonic anemometer (Solent Research R3, Gill Instruments, Lymington, UK) and an infrared gas analyser (model Li-7000, LiCor Inc., Lincoln, NE, USA). The eddy covariance system and procedures were those currently used in the Carboeurope IP and Fluxnet networks (Moncrieff et al., 1997; Grelle and Lindroth, 1996; Aubinet et al., 2000). Meteorological measurements were averaged every 30 min. They included air temperature and humidity (RHT2, Delta-T Devices Ltd., Cambridge, UK) at a height of 1.3 m. Global photosynthetically active (PAR Quantum Sensor SKP 215, Skye Instruments Ltd., UK) and global and diffuse photosynthetically active (Sunshine sensor type BF3, Delta-T Devices Ltd., Cambridge, UK) radiation was measured at a height of 2.7 m. Details of the eddy covariance system and meteorological measurements are given in Moureaux et al. (2006).

The crop under study was winter wheat (*Triticum aestivum* L., cv Dekan). It was sown on 14 October 2004, following a sugar beet crop (*Beta vulgaris* L.) harvested on 29 September 2004. No ploughing was done between the two crops, but minimum tillage with a rotating harrow prepared the soil for seedling and mixed green residues of sugar beet into a 10 cm layer of soil. The field management schedule is summarised in Table 1. Two herbicide treatments were applied, on 18 March and 11 May. Nitrogen was applied in four fractions (on 22 March and 12 April with a urea ammonium nitrate solution, and on 12 and 30 May with NH_4NO_3). There was only one fungicide treatment, on 19 May. The crop was harvested on 3 August.

2.2. Measurements

Measurements were made at the site at different spatial and temporal scales. They included: regular dry-matter sampling during the growth period, continuous eddy covariance measurements, continuous soil respiration measurements and leaf scale assimilation measurements. We give details below on the measurements used in this study.

2.2.1. Vegetation measurements

Photosynthetic photon flux density (PPFD) absorption by the crop was measured using a ceptometer (Sunscan, Delta-T

Table 1 – Description of the treatments applied in the field during the winter wheat growing season

Date	Treatment
14/10/2004	Sowing
18/03/2005	Weeding (1.5l IP–1.5l Verigal)
22/03/2005	First application of liquid nitrogen (45 units/ha)
12/04/2005	Second application of liquid nitrogen (35 units/ha)
11/05/2005	Weeding (40 g Harmony–25 g Gratil)
12/05/2005	First application of NH_4NO_3 (40.5 units/ha)
30/05/2005	Second application of NH_4NO_3 (81 units/ha)
19/05/2005	Fungicide treatment (1l Opus – 0.5l Amistar)
03/08/2005	Harvest

Devices, Cambridge, UK). Measurements were performed in four different plots every 10 days between 12 May and 15 July 2005. The ceptometer was placed successively above the crop and at the soil surface. In each plot, 20–30 replicates were taken.

The total vegetation, green leaf, stem and ear areas were deduced from sampling. Each week between 22 April and 19 July 2005 all the plants were sampled from a row 30–50 cm long. Their green leaf surface was measured using a picture analyser (WinDIAS, Delta-T Devices, Cambridge, UK). The stem and ear (from 31 May) length and diameter were also directly measured. Green leaf area index (GLAI), stem area index (SAI) and ear area index (EAI) were deduced from these measurements by multiplying the respective average surfaces per tiller by the number of tillers per soil surface unit. For light interception calculations, the surface considered for stems and ears was the cross-section; for the estimation of the CO_2 flux exchange area, the surface considered was the external area. Total vegetation area index (VAI) was calculated by adding the leaf, stem and ear area indexes.

Finally, the leaf stomatal ratio, which is needed to deduce the assimilation from the measurement chamber, was determined by direct counting. Three plants were collected and two leaves were taken from each of them. On each leaf surface, three microscopic cuts were made on which the stomata number was counted.

2.2.2. *Photosynthesis measurements*

Photosynthesis was measured in the field, at the leaf scale, using an open gas exchange system (Li-Cor 6400, Li-Cor Inc., Lincoln, NE, USA) equipped with a modulable light source (6400-02B LED). The leaf was inserted into the chamber and saturated by light (1700 $\mu mol\ m^{-2}\ s^{-1}$) for about 25 min so that stomatal conductance reached equilibrium. The light was then reduced from saturation point to 500 $\mu mol\ m^{-2}\ s^{-1}$ by steps of 200 $\mu mol\ m^{-2}\ s^{-1}$, and then to dark (0 $\mu mol\ m^{-2}\ s^{-1}$) by steps of 100 $\mu mol\ m^{-2}\ s^{-1}$. At each step, there was a 5-min delay before the measurements were taken in order to make photosynthetic apparatus adjustments to the light regime. The measurements were then repeated three times. Net assimilation (*A*, $\mu mol\ CO_2\ m^{-2}\ s^{-1}$) to photosynthetic photon flux density (PPFD, Q, $\mu mol\ m^{-2}\ s^{-1}$) responses (*A*–Q curves) were deduced from these measurements. Measurements of leaf temperature, leaf-to-air vapour pressure difference (D_l), intercellular CO_2 concentration and stomatal conductance were also performed. The measurement procedure was as prescribed by the system manual (Li-Cor, 2003). Leaf temperature, air humidity and CO_2 concentration in the chamber were kept constant throughout the curve measurement.

Relevant parameters (A_s, the net and G_s, the gross assimilation at saturating light [$\mu mol\ CO_2\ m^{-2}\ s^{-1}$], α, the quantum yield [$\mu mol\ CO_2\ \mu mol^{-1}$ photons] and R_d, the dark respiration [$\mu mol\ CO_2\ m^{-2}\ s^{-1}$]) were deduced from the measurements by fitting a non-linear equation on measured A–Q curves. We used the Misterlich equation (Dagnelie, 1991):

$$A = (A_s + R_d)\left(1 - \exp\left\{\frac{-\alpha Q}{(A_s + R_d)}\right\}\right) - R_d = G_s\left(1 - \exp\left\{\frac{-\alpha Q}{G_s}\right\}\right) - R_d \quad (1)$$

This equation was preferred to the classical rectangular hyperbola because it saturates at a lower PPFD and leads to more realistic saturation assimilation values (Aubinet et al., 2001). As a result, saturation assimilation and quantum yield values were typically 30 and 20% lower when deduced by Eq. (1) than by a classical Michaelis Menten equation. The fitting was obtained by non-linear regression using the Marquart–Levenberg method.

Homogeneity of the A–Q response in the crop was evaluated by repeating measurements at different leaf levels from the same tiller, on different tillers from the same plant and on different plants. The relationship between A and Q curve characteristics and season or climate was also investigated by repeating the measurements on 14 separate days characterised by different meteorological conditions and crop development stages. The impact of senescence on the leaf photosynthetic capacity was assessed by conducting measurements on both green and senescent leaves. Leaf respiration measurements were also performed during the night. The measurement chronology is summarized in Table 2.

2.2.3. *Air humidity characterisation*

In this paper, a distinction is made between the air saturation deficit (D_s) and the leaf to air vapour pressure difference (D_l). Both are defined as a difference between a saturated vapour pressure and actual air vapour pressure. However, in D_s, the saturated vapour pressure is taken at the air temperature while in D_l, it is taken at the leaf temperature. D_s was directly measured at the field scale by the meteorological station while D_l was measured at the leaf scale by the open gas exchange system. No direct D_l evaluation at canopy scale was available. It was thus deduced from D_s and from a leaf energy balance assessment as shown below (Section 3.4).

2.3. *Extrapolation model description*

2.3.1. *General procedure*

A model was developed in order to extrapolate A–Q curves from the leaf scale to the crop scale and to the whole vegetation season. First, the vegetation was divided into 10 layers of equal VAI. In each layer i, the incident PPFD (Q_i), was deduced from the PPFD measurements in taking into account the absorption by the vegetation situated above the middle of the *i* layer. The leaf gross assimilation (G_i) was then computed for each layer by introducing Q_i into a relationship derived from (1):

$$G_i = G_s\left(1 - \exp\left\{\frac{-\alpha Q_i}{G_s}\right\}\right) \quad (2)$$

The crop gross assimilation was computed every 30 min by multiplying G_i by the area index of photosynthesizing vegetation in the layer (phototsynthetic area index, $PsAI_i$) and by summing each layer contribution. Finally, daily and yearly GPP were obtained by a summation of the half-hourly values.

2.3.2. *Calibration*

The model calibration required the description of the incident PPFD in each layer, of the PsAI distribution in the crop and a parameterisation of the photosynthetic parameters G_s and α.

Table 2 – Chronology of leaf scale measurements. F1 corresponds to flag leaf, F2 to last but one leaf, F3 to last but two leaf; 'senescent' means that the leaf has begun the death process but still photosynthetizes, and 'necrosed' means that the leaf cells are dead and therefore no more photosynthesis is observed

Date	Strategy	Leaf level	Note
1/05/2005	2 leaves from the same tiller	F2–F3	
5/05/2005	2 leaves from the same tiller	F2–F3	
15/05/2005	2 leaves from the same tiller	F2–F3	
19/05/2005	2 leaves from 2 different tillers of the same plant + exploratory respiration	F2	
28/05/2005	Study of 1 necrosed leaf in comparison with 1 green F1	F1–F3	3 measurements on a necrosed leaf (F3)
9/06/2005	2 leaves from 2 different plants	F2	
10/06/2005	2 leaves from the same tiller	F1–F2	
15/06/2005	2 F2, 1 F3 and 1 F1 from different plants	F1–F2–F3	F3 and 1F2 were damaged
22/06/2005	4 leaves from 2 different tillers	F1-F2	
10/07/2005	1 green F1 + back on the tiller of the 15/05/2005	F1–F2	Tiller of the 15/05/2005: F2 (1 measurement on necrosed part and 1 measurement on green part) + F1
13/07/2005	1 A–Ci + 1 A–Q curves on the same leaf	F1	
14/07/2005	1 green F1 + back on the tiller of the 05/05/2005 + 1 senescent leaf	F1	Tiller of the 05/05/2005: senescent F1
16/07/2005	1 green F1 and 1 damaged F1 + nocturnal measurements	F1	Night: 2 green leaves, 1 necrosed leaf and 2 senescent leaves
23/07/2005	Necrosed and senescent leaves	F1	

When possible (from 12 May to harvest), Q_i was directly estimated from ceptometer measurements as:

$$Q_i = Q_0 \tau^{2i-1/20} \quad (3)$$

where Q_0 is the incident PPFD above the crop (μmol m^{-2} s^{-1}), measured every 30 min by the micrometeorological station and τ represents the transmission factor of the whole crop, estimated as the ratio of the incident PPFD below and above the crop, measured with the ceptometer.

From emergence to 12 May, ceptometer measurements were not available due to the short height of the crop. Q_i was thus deduced from the Beer's law (Monteith and Unsworth, 1990):

$$Q_i = Q_0 \exp(-kV_i) \quad (4)$$

where k is the extinction coefficient and V_i is the cumulated VAI of the layers above the layer i (m^2 m^{-2}). The extinction coefficient k was evaluated by comparing Q_i estimations using the two approaches on two days (10 and 12 May) where both ceptometer measurements and leaf area measurements were available. This gave $k = 0.63$.

The evaluation of the PsAI distribution presents some difficulties that are specific to cereal crops. First, photosynthesizing areas do not relate only to leaves but also to stems and ears. However, the photosynthetic activity of these elements probably differs from those of the leaves. Second, it depends on the yellow organ distribution, which becomes predominant at the end of the season.

Stem and ear photosynthetic activity could not be measured directly as the measurement chamber did not allow photosynthesis measurements on thick elements. The possible impact of these vegetation parts on the GPP was thus assessed by comparing two hypotheses: the first one assuming that their photosynthetic activity was similar to that of the leaves and the second one that it was zero. Finally, a more realistic evaluation of the photosynthetic capacity of stem and ears was proposed by comparing model results with GPP eddy covariance estimates.

For the yellow organ distribution, we assumed a progressive development of the yellow organs from the bottom to the top of the canopy, which is the most realistic scenario in cereal crops. However, as the yellowing progression was not directly measured during the experiment, we evaluated the possible impact of another progression by also testing a homogeneous yellowing distribution.

Finally, the model required a description of G_s and α evolution according to the principal driving factors (time and/or climatic variables) and an evaluation of the vertical distribution of these parameters in the crop. This was obtained only after having thoroughly analysed the measurements made at leaf scale. Consequently, this part is discussed below (Section 3.4).

3. Experimental results

3.1. Climatic conditions

The mean daily climatic measurements results are given in Fig. 1. During winter the air temperature (T_a) was always below 10 °C and frost occurred twice: in December and at the end of February/early March. However, T_a never fell below −5 °C (Fig. 1a). Winter was also characterised by low air saturation deficit (D_s, Fig. 1b), low photosynthetic photon flux density (PPFD, Fig. 1c) and well-watered soil (Fig. 1d). In contrast, the end of spring was marked by much drier conditions: at the end of June, T_a reached 25 °C (Fig. 1b), D_s peaked to about 12 hPa (Fig. 1c) and the soil water content fell to 0.12 m^3 m^{-3} (Fig. 1d). These conditions were fairly representative of the regional averages for the previous 10 years, except for the water deficit, which was a bit more pronounced.

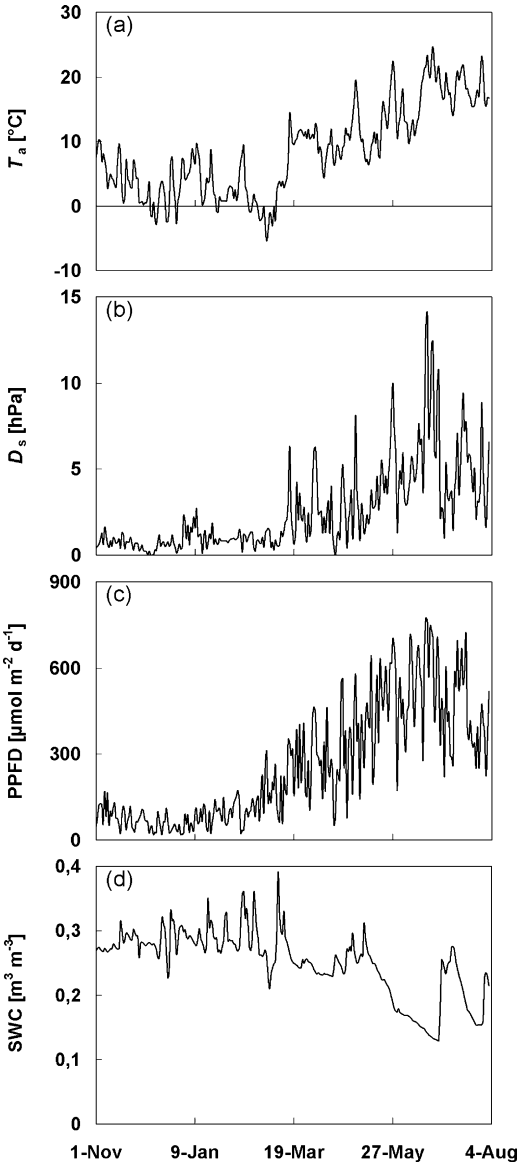

Fig. 1 – Seasonal evolution of climatic variable daily means from 1 November to 2 August: (a) air temperature, (b) air saturation deficit (D_s), (c) photosynthetic photon flux density (PPFD) and (d) soil water content at 5 cm (SWC).

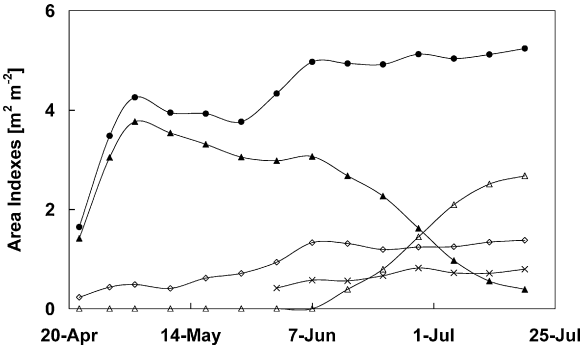

Fig. 2 – Seasonal evolution of the vegetation part area indexes: total vegetation (solid circles), green leaves (solid triangles), stems (open circles), ears (crosses) and yellow leaves (open triangles).

3.2. *Plant development*

Until May–June, the crop had not been submitted to any stress. Emergence occurred 2 weeks after sowing. Tillering (stages 21–30 on Zadoks scale; Zadoks et al., 1974) started in early March and ended in mid-April. At this point the VAI was about 1.6 and it then increased rapidly until early May (Fig. 2). In early May, a decrease in GLAI was observed that corresponded to stem elongation (Fig. 2). During this period, a few tillers on each plant (less than three per plant) exerted their dominance over the others, which regressed and died. The temporary reduction in GLAI was therefore because the growth of the dominant tillers did not compensate for the reduction of tillers per unit of soil surface. Flag leaf emergence occurred in mid-May (stage 37 on Zadoks scale). The subsequent VAI increase was due mainly to stem and ear development (ear emergence occurred in early June, stage 50 on Zadoks scale) (Fig. 2). On 7 June, VAI reached its maximum and then remained fairly constant until the end of July (Fig. 2). However, plant senescence began from early June, with the leaves at the bottom of the plants beginning to turn yellow. This explains the GLAI decline despite a constant VAI. The daily yellow leaf area index (YLAI) in Fig. 2 was not directly measured but was evaluated as the difference between the GLAI value on 7 June and the GLAI value of the day. At the end of July, the GLAI fell to zero and the YLAI reached about 50% of the VAI. The total SAI and EAI remained fairly constant during June and July and constituted about 25 and 15% of the VAI, respectively. At emergence, the ears rapidly reached their maximum size, and their further increase in diameter due to grain development was fairly negligible, which explains the EAI stability in June and July.

Compared with the regional average, crop development followed the standard rate until stage 57 on Zadoks scale (3/4 of inflorescence emerged), but after late May a more rapid development than average was observed, the drought accelerating leaf senescence and ear maturation. The drought effect was probably enhanced by the early sowing and the 'no ploughing' practice. At the end of July, when the ears were mature, precipitation occurred (results not shown), increasing the grain humidity and delaying the harvest date.

3.3. *Assimilation to light responses*

3.3.1. *Homogeneity and impact of senescence*

Thirty-two valid A–Q curves were produced between 1 May and 23 July 2005. As stated earlier (Section 2.2.2), measurements were performed at different plant levels (the three upper leaves) and on leaves at different senescence stages.

For green leaves, no significant differences between A–Q curves were observed between the different plants, between the tillers of the same plant or between the three upper leaves. This accords with the results reported by Veneklaas and Van Den Boogaard (1994), who did not find any effect of leaf age on photosynthesis in two varieties of winter wheat.

Fig. 3 presents three A–Q curves produced under the same meteorological conditions on three leaves at different senes-

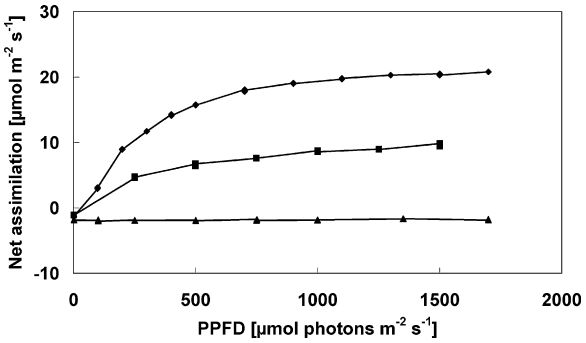

Fig. 3 – Three examples of A–Q curves corresponding to leaves at different senescence stages: green leaves (diamonds), yellow leaves at the beginning of senescence (squares) and dead leaves (triangles).

cence stages. In the case of the green leaf, the classical increase of A with Q was observed, with saturation reached at about 20 µmol CO_2 m^{-2} s^{-1} at large radiation. The maximal value of A_s observed was 21.4 µmol CO_2 m^{-2} s^{-1} on 28 May 2005. These values are of the same order of magnitude as those reported in the literature: Soegaard and Thorgeirsson (1998) reported 23.7 µmol CO_2 m^{-2} s^{-1} on spring wheat with a non-rectangular hyperbola and Rodriguez et al. (1998) reported 22.8 and 29.4 µmol CO_2 m^{-2} s^{-1} on the leaves of winter wheat using Eq. (1). The latter results were obtained during the tillering phase, which could explain these larger values.

A similar relationship was observed for the yellow leaf but with a lower saturation value, revealing a fall in leaf photosynthetic capacity. Finally, the dead leaf did not photosynthesize, but was still able to respire.

3.3.2. G_s response to driving variables

The relationship between the parameters extracted from the different A–Q curves and possible driving variables were analysed. In particular, as shown in Fig. 4, we gathered the distributions of G_s, α and R_d, with time, leaf temperature (T_l) and leaf-to-air vapour pressure difference (D_l). It is clear that G_s declined with the three variables (Fig. 4a–c). In the three cases, the trend was found to be significant ($P = 0.0026$, 0.0060 and 0.0047, respectively). However, these correlations did not each necessarily represent a real dependency because the three variables were not independent from each other. First, D_l is by definition related to leaf temperature and, second, these two variables were correlated with time as dry and hot conditions were observed mainly at the end of the observation period. We supposed that the G_s decline with D_l was probably the most representative of a real mechanism. Indeed, stomatal closure is known to occur under high D_l (e.g., Tewolde et al., 1993; Leuning, 1995), inducing leaf assimilation reduction. In these conditions,

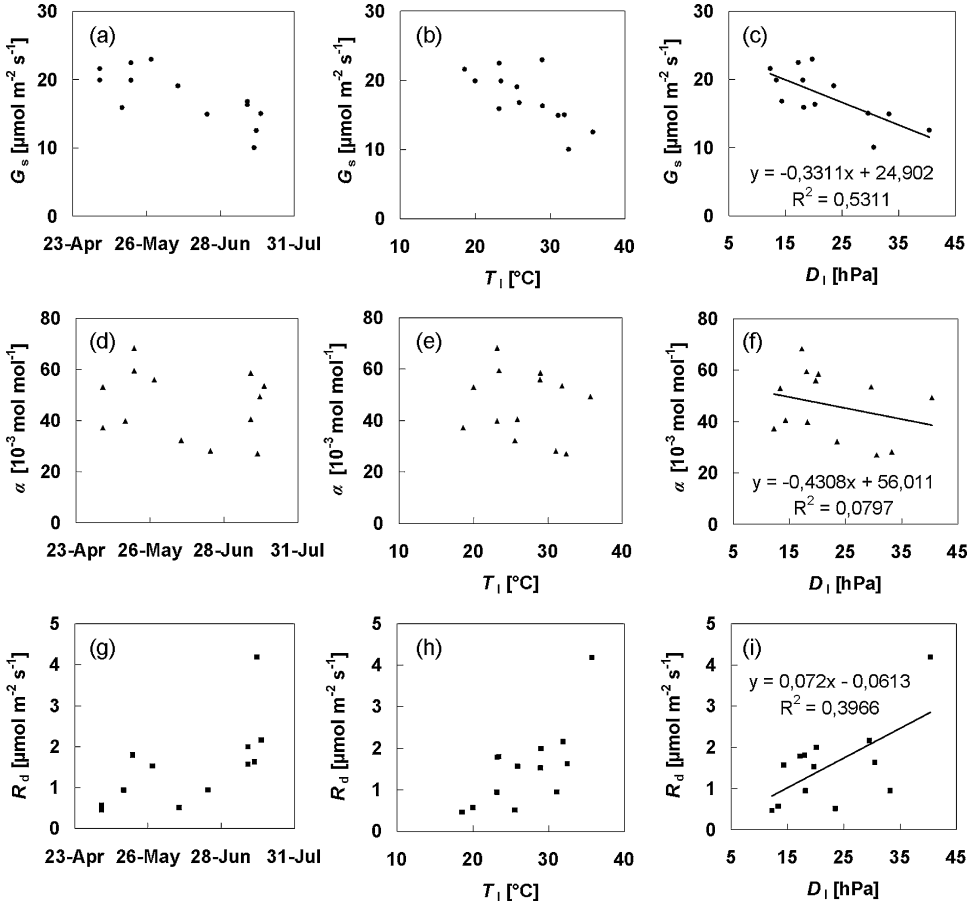

Fig. 4 – Relationship between gross assimilation at saturating light (G_s), dark respiration (R_d) and quantum yield (α) with time, leaf temperature (T_l) and leaf to air vapour pressure difference (D_l).

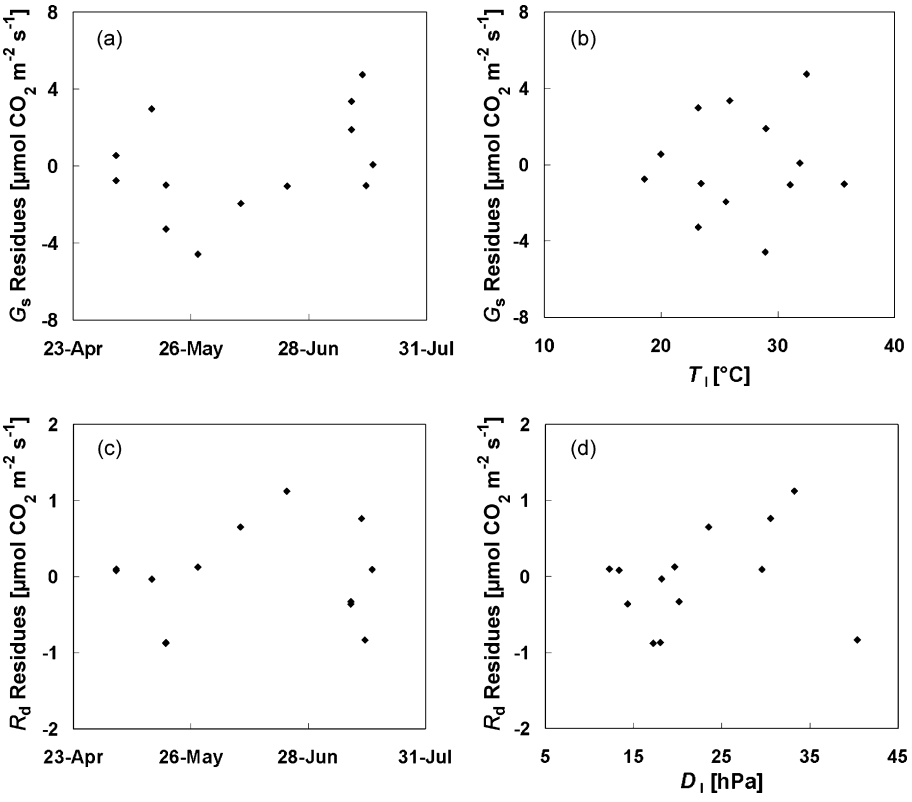

Fig. 5 – Relationship between the residues of the G_s response to D_l with time (a) and leaf temperature (b). Relationship between the residues of the R_d response to leaf temperature with time (c) and with leaf to air vapour pressure difference (d).

the responses of G_s to time and air temperature appear rather as the result of an artefact; indeed, the residues of the linear regression of G_s to D_l were not correlated to time and air temperature (Fig. 5a and b). The absence of correlation between residues and air temperature confirms the suggestion by Schulze and Hall (1982) that assimilation responses to high temperatures have often been confounded with the response to D_l. A modulation of the G_s to D_l response by soil water potential could also be possible, as shown by Xue et al. (2004). However, our measurements were not numerous enough and did not encompass a sufficiently large soil water potential range to allow us to highlight such an effect.

Finally, it should be noted that, due to the porometer regulation, which requires drying the air before pushing it into the chamber, the drought conditions were probably exaggerated by the chamber compared with the ambient air. However, the D_l values measured by the porometer reflect the conditions really underwent by the leaf portion whose assimilation is measured. It is therefore reasonable to think that, if the whole field were subjected to the same conditions, it would undergo the same assimilation decrease. Consequently we consider that the responses to D_l that were observed at leaf scale could be extrapolated at crop scale provided that a convenient estimation of D_l is given.

3.3.3. *α response to driving variables*

Quantum yield did not exhibit any trend with climatic variables or with time (Fig. 4d–f). The α values varied from 0.027 to 0.068 µmol CO_2 µmol^{-1} photons, with an average of about 0.046 µmol CO_2 µmol^{-1} photons and a standard error always lower than 0.002. These values are of the same order of magnitude as those reported in the literature: values of 0.042, 0.03–0.05 and 0.062 µmol CO_2 µmol^{-1} photons were reported, respectively, for winter wheat (Soegaard and Thorgeirsson, 1998), spring wheat (Rodriguez et al. (1998) and on average for C3 crops (Ruimy et al., 1995)). However, this last-mentioned value was derived from a Michaelis Menten regression, which gives larger estimates of this parameter, as stated earlier.

3.3.4. *R_d response to driving variables*

An increase of R_d with time, temperature and D_l was also observed (Fig. 4g–i). Here again, the three trends are significant ($P = 0.0314$, 0.0073 and 0.0211, respectively) but, as the three variables are linked as explained above, some of the correlations are expected to be artificial. In this case, the most probable response is that to temperature, as widely reported in the literatures (see in particular Lloyd and Taylor, 1994; Janssens et al., 2003). We therefore retained leaf temperature as the most important driving variable. Residues of the relationship of R_d to temperature not being found correlated to time and leaf to air vapour pressure difference (Fig. 5c and d), the relationships in Fig. 4 were again interpreted as an artefact and not taken into account.

3.4. *Result synthesis: G_s and α calibration*

The preceding results may be synthesised in order to allow parameterisation of the photosynthesis parameters. First, as

the parameters were found not to depend on the leaf position (§ 3.3.1) or age (§ 3.3.2–3.3.4), they were supposed to be similar for all green leaves.

In Section 3.3.1 (Fig. 3), yellow leaves were found to still assimilate, albeit at a lower rate, suggesting a progressive drop in assimilation with the senescence stage. This was, however, difficult to model, mainly because of the high degree of subjectivity in defining the senescence stage. With regard to this difficulty, yellow leaf assimilation was considered as equal to zero.

Following the discussion in Section 3.3, the sole driving variable retained for G_s parameterisation was the leaf to air vapour pressure difference. The relation between D_l and G_s was approximated by a linear model. Least squares regression on the experimental points of Fig. 4c gave:

$$G_s = -0.331 D_l + 24.905 \quad (5)$$

with a R^2 equal to 0.53 and a P value of 0.0047. In order to scale up this relation, D_l should be known at the crop scale. It was stated above that this variable was not directly available but could be deduced from the leaf energy budget. We can indeed write:

$$D_l = e^*(T_l) - e_a \quad \text{with} \quad T_l = T_a + \frac{Hu}{\rho C_p u_*^2} \quad (6)$$

where e_a is the air vapour pressure and $e^*(T)$ is the saturation vapour pressure at temperature T, T_l (°C) and T_a (°C) are the leaf and air temperatures, respectively, H (Wm^{-2}) is the sensible heat, u_* and u (m s^{-1}) are the friction and average velocity, respectively, ρ is the air density (kg m^{-3}) and C_p the air specific heat (J kg^{-1} K^{-1}).

However, D_l cannot be estimated when sensible heat and friction velocity are not available. It could therefore be relevant to evaluate the error made when approximating D_l by D_s. In practice, we found that at our site the differences between leaf and air temperatures were lower than 1 °C for 50% of the daytime and lower than 4.5 °C for 95% of the daytime, so that the difference between D_l and D_s was often small. The impact on the GPP of this approximation will be given in the sensitivity analysis.

Facing with the difficulty to scale up the G_s to D_l response, one could be tempted to replace Eq. (5) by a regression of G_s with the air saturation deficit measured by the meteorological station that could be easier to scale up. However this is not recommended as the air saturation deficit is not representative of the drought conditions to which the leaf was subjected in the porometer chamber. As a consequence this approach would lead to an overestimation of the crop water stress and to an underestimation of the crop GPP. The impact of the error made by doing this will also be evaluated in the sensitivity analysis.

Even if R_d does not appear explicitly in the model, its evaluation was required in order to determine α. Following the discussion in Section 3.3, R_d was parameterised as a function of leaf temperature. We used the Van't Hoff equation (1898) (Lloyd and Taylor, 1994):

$$R_d = R_{d25} Q_{10}^{(T_a - 25/10)} \quad (7)$$

where R_{d25} is the dark respiration (μmol m^{-2} s^{-1}) at 25 °C, Q_{10} is the sensitivity of respiration to temperature and T_a is the air temperature (°C). Regression gave R_{d25} = 1.10 (S.E. = 0.22) and Q_{10} = 2.83 (S.E. = 0.75) with a R^2 equal to 0.59.

As no clear relationship of α with climatic and non-climatic parameters was found, it was fixed as a constant. Its value was computed in order to reduce uncertainty for this parameter as much as possible. All the A–Q curves measured on green leaves were gathered and a model combining Eqs. (1), (5) and (7) was fitted on these data. As a result, α was the unique parameter to adjust in a non-linear regression between net assimilation and PPFD, air temperature and leaf to air vapour pressure difference. All variables were measured by the porometer. This regression gave α equal to 0.0452 μmol CO_2 μmol^{-1} photons, with a standard error of 0.0009.

4. Model results

4.1. *Seasonal flux evolution*

The general evolution of GPP estimated with our model is presented in Fig. 6a, along with those provided by eddy covariance measurements (Moureaux et al., in press). For this presentation, we used the best model estimate obtained by adjustment of the eddy covariance data for the development and maturation periods. As a result, the summed GPP were equal for the two estimates for these periods. They were 1570 g C m^{-2}. Except in early spring, scaled-up and eddy covariance estimates of GPP matched each other quite closely (slope of the regression = 1.13, R^2 = 0.94). This high level of

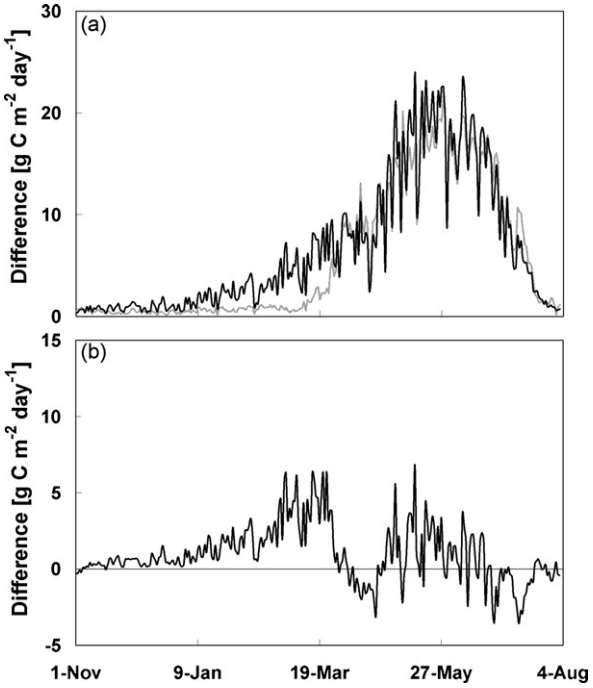

Fig. 6 – (a) Seasonal evolution of the winter wheat crop daily GPP estimated with the scaling up model (solid line) and with eddy covariance measurements (grey line); (b) seasonal evolution of the difference between the model and the measurements.

agreement related not only to the seasonal trend, but also to day-to-day variations, as observed particularly at the end of the season. Before early March, the assimilation was slightly positive in both cases and increased sharply from early March until early May, which corresponds to the phase of intense crop development. Maximal values were reached in May, after which the GPP fell abruptly until the end of the season, when it reached zero. The disagreement between the two estimates that appears in winter and spring is discussed later.

4.2. *Sensitivity analysis*

4.2.1. *Stem and ear assimilation*

First, in order to assess the possible impact of ear and stem contributions to GPP, the model was run three times using three hypotheses to estimate the PsAI: (A) only the leaves are photosynthesising (i.e., PsAI = GLAI); (B) stems and leaves photosynthesise at equivalent rates (PsAI = GLAI + SAI); (C) stems, leaves and ears photosynthesize at equivalent rates (PsAI = GLAI + SAI + EAI). Before May, the three runs gave the same results as the stems and ears were not well developed (cf. Fig. 2). Paired t tests performed on the data after the beginning of May showed that the differences between the three runs were significant (cf. Fig. 7) ($P < 0.0001$). From mid-May until the end of the season, the three situations clearly differed, with maximum values of 21, 28 and 36 g C m^{-2} day^{-1} for situations A, B and C, respectively. In addition, the maximum was reached later in the last two situations (8 June) than in the first (12 May), as the stem and ear development occurred later in the season while the green leaf area was already decreasing due to crop senescence. Cumulated GPP was highly sensitive to this parameter as the inclusion of the stems in the photosynthetically active organs led to an increase of 40% in the initial GPP estimation and the inclusion of the ears to an additional increase of 15%. Compared with the eddy covariance GPP estimations, the extrapolation scheme underestimated the GPP in situation A and overestimated it in situations B and C. This suggests that the stem and ear contributions to assimilation are clearly important but that these organs probably present a lower photosynthetic capacity than the leaves. The best agreement with eddy covariance measurements was obtained by taking

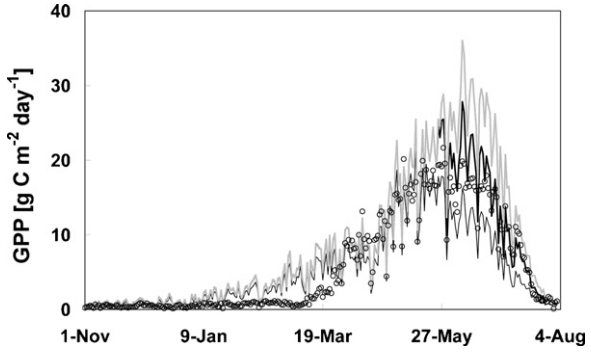

Fig. 7 – Comparison between the GPP seasonal evolutions simulated using three PsAI scenarios: (A) only leaves (thin line); (B) leaves and stems (solid line); or (C) leaves, stems and ears (grey line) are photosynthesizing. Open circles correspond to eddy covariance measurements.

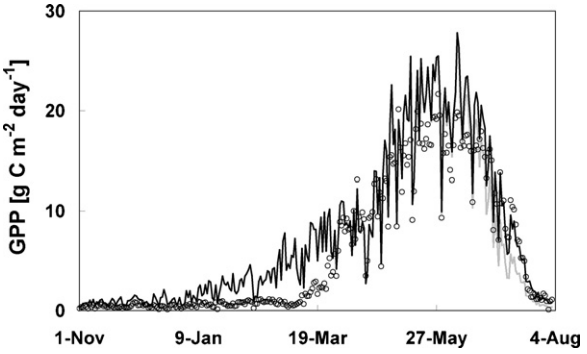

Fig. 8 – Comparison between the GPP seasonal evolutions simulated postulating a homogeneous (grey line) or a bottom (solid line) distribution of yellow organs, assuming that leaves and stems photosynthesize. Open circles correspond to eddy covariance measurements.

hypothesis B and assuming a stem photosynthetic capacity equal to 63% of that of leaves. Further measurements made in 2007 on the same field confirmed that the stems photosynthesize but at a lower rate. It was used in the following simulations. This result clearly needs to be confirmed by further A–Q curves made on stems in the field.

4.2.2. *Spatial distribution of yellow parts*

In the preceding model, yellowing was supposed to progress from the crop bottom to the top (bottom distribution). However, even if highly probable, this hypothesis was not checked experimentally. Its impact was therefore tested by comparing the preceding simulations with those of a model submitted to a similar yellowing in all the crop layers. The difference between the two models was about 7–9%, depending on the situation. The impact of the yellowing distribution was significant only after early June (the paired t test gave $P < 0.0001$), the GPP being always higher for the bottom rather than the homogeneous repartition (Fig. 8). This is because, with the bottom distribution, a larger part of the upper leaves, which take greater advantage of sun radiation, remained photosynthetically active for a longer time. The difference in yellowing distribution did not severely affect the maximum daily assimilation values (27 and 28 g C m^{-2} day^{-1} for homogeneous and bottom distributions, respectively). A comparison of these trends with eddy covariance GPP showed that the bottom distribution gave a more realistic evolution of the GPP at the end of the season, confirming the former hypothesis.

4.2.3. *Regression parameters*

In order to study the sensitivity S of annual GPP to the model parameters (P), we used the following definition:

$$S = \frac{\Delta G/G}{\Delta P/P} \tag{8}$$

where Δ represents an absolute variation and the parameter P may represent saturation gross assimilation, dark respiration or quantum yield. This ratio is dimensionless. The impact of each parameter uncertainty on the annual GPP was therefore

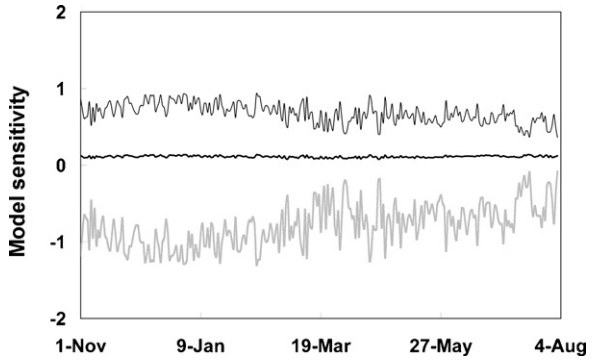

Fig. 9 – Seasonal evolution of the model sensitivity to parameter uncertainties: G_s (grey line), α (thin line) and R_d (thick line).

computed by multiplying the former with the corresponding sensitivity.

The normalized sensitivity of annual GPP to G_s, α and R_d were about −0.65, 0.6 and 0.11, respectively (Fig. 9). As the uncertainties on these parameters (Standard Errors) were 5, 2 and 10%, respectively (§ 3.4), their impact on the annual GPP was about 4%, slightly larger than 1 and 1%, respectively.

Surprisingly, the sensitivity to G_s was negative, meaning that an increase of this parameter caused a GPP decrease. This can be explained by the calibration procedure: as α was deduced from a regression after G_s had been fixed, a greater G_s value would induce a lower α value. This had more impact on the GPP than the G_s increase itself, as radiation was not saturating for most of the canopy most of the time. The fact that the parameters are estimated in reference to α explains that the sensitivities are larger in absolute value in winter and spring than in summer. Indeed, during these periods, leaves were rarely saturated by light and therefore their assimilation rate was determined more by quantum efficiency than by other parameters.

The last point of this sensitivity analysis concerns the impact of the way the response of G_s to air humidity is parameterised. We found, on the one hand, that the error made by approximating D_l by D_s in the scaling up procedure led to a GPP overestimation of 20 g C m^{-2}. On the other hand, the error made by replacing Eq. (5) by a G_s to D_s regression led to a GPP underestimation of 70 g C m^{-2}. The impacts of these errors on GPP went thus in the same way as predicted but their importance were limited. This is because the drought condition underwent by the crop were quite smooth and limited in time. These impacts could be more important in crops subjected to more arid conditions.

4.3. *Comparison with eddy covariance measurements*

The preceding analysis suggested that more realistic assimilation estimations were obtained when assuming that stems assimilate at a lower rate than leaves (63%) and that the yellowing progressed upwards from the lower parts of the canopy. The evolution of the GPP extrapolated from leaf scale measurements using these hypotheses and deduced from eddy covariance estimations is presented in Fig. 6a, as well as the difference between them (Fig. 6b).

We will now focus on these differences. First, it seems clear that before April the scaled-up GPP estimates were systematically higher than the eddy covariance estimates. This is because the extrapolation scheme does not take account of the photosynthesis response to low temperatures. Clearly, the eddy covariance deduced estimate was more realistic here: negative air temperatures were observed between mid-February and early March, which hindered any photosynthetic activity. This effect cannot be taken into account by the extrapolation scheme because no leaf scale measurements were performed during this period. The overall impact of this overestimation on total GPP was 270 g C m^{-2}.

From April until harvest, the average difference between the two GPP estimates was zero as a result of the stem photosynthetic capacity adjustment. The root mean squared difference between the two estimates was 1.9 g C m^{-2} d^{-1} which is about 16% of the daily average GPP. It was mainly negative in April and July and positive in June and May, suggesting that the extrapolation scheme overestimated the GPP in the latter months and underestimated it during the former months. Underestimation in July could be due to neglecting the photosynthetic contribution of the 'yellow' organs. Indeed, in this scheme, only the green organs were taken into account in the photosynthetic area, whereas we showed earlier (Fig. 3) that senescent organs could still assimilate, albeit at a lower rate. The overestimation in May and June was positively correlated with the GPP itself and with radiation, and was not related to D_l.

5. Conclusion

A model was developed in order to scale up assimilation measurements from leaf to canopy scale in a winter wheat crop. The model was based on porometer measurements made in the field during the growth period. These measurements showed an increase in assimilation with PPFD of dark respiration with temperature and a decrease in saturating assimilation with leaf to air vapour pressure difference. The model correctly reproduced the GPP during the development and maturation period, but not during winter because it did not take account of the photosynthesis reduction at low temperature. An analysis was developed in order to determine the most important causes of uncertainty affecting these results.

The most important cause of uncertainty resulted from the assimilation of stems and ears. A model considering only assimilation by leaves underestimated the GPP by 23%, whereas a model considering stems as organs assimilating at the same rate as leaves increased the GPP by about 600 g C m^{-2}, leading to a 14% overestimation GPP. These two estimates bracketed the eddy covariance estimate, suggesting that the reality lay between these two extreme hypotheses. The best agreement with the eddy covariance estimate was obtained by assuming a stem assimilation equal to 63% of leaf assimilation, which was found compatible with further leaf scale measurements. More generally, this result shows that a correct determination of stem and ear assimilation is critical when scaling up wheat (and, more generally, cereal) assimilation from leaf to canopy scale.

The second cause of uncertainty was linked to the yellow organ distribution. In particular, it was shown that a model with a homogeneous repartition of the yellow organs gave GPP estimates 7–9% lower than the model, postulating a bottom yellowing distribution. This suggests the importance of better evaluation of yellow organ progression and photosynthetic capacity in the field. Measurements with a chlorophyll meter would be an option for clarifying this area of assimilation. Hanan et al. (2005) reported a similar problem, showing that their land surface model (SiB2) overestimated crop photosynthetic uptake at the end of the season because they had not taken into account the physiological senescence.

The third cause of uncertainty is linked to the winter period. From January to March, the scaling up overestimated the GPP because the assimilation reduction at low temperatures was not taken into account by the model. The resulting error was about 10% of the GPP. Such an underestimation is specific to winter species and would not be so critical for spring species that do not have to contend with low temperatures for long periods. The problem could be easily solved by performing some A–Q curves in winter conditions and introducing an assimilation response to low temperature in the model.

Finally, the impact of the A–Q curve parameter uncertainties was found to be the weakest, not exceeding 4%. Rodriguez et al. (2000) reported that for well-irrigated conditions a simple approximation based on a light response curve avoiding the calculation of the coupling between photosynthesis and stomatal conductance could be used. This study confirmed that this is possible once a careful identification of photosynthesizing organs and monitoring their evolution has been performed at the site.

Acknowledgements

Funding for this project was provided by the Communauté française de Belgique (Direction générale de l'enseignement non-obligatoire et de la recherche scientifique – Action de Recherche Concertée – Convention no. 03/08-304) and by the European Commission (Carboeurope IP—contract GOCE-CT-2003-505572, IMECC contract 026188). The authors are grateful to Alain Debacq for the eddy covariance system and micrometeorological station maintenance and to the Unité de Phytotechnie tempérée (Fusagx) staff for undertaking the crop monitoring.

REFERENCES

Anthoni, P.M., Knohl, A., Rebmann, C., Freibauer, A., Mund, M., Ziegler, W., Kolle, O., Schultze, E.D., 2004. Forest and agricultural land-use-dependent CO_2 exchange in Thuringia, Germany. Glob. Change Biol. 10, 2005–2019.

Aubinet, M., Grelle, A., Ibrom, A., Rannik, Ü., Moncrieff, J., Foken, T., Kowalski, A.S., Martin, P.H., Berbigier, P., Bernhofer, C., Clement, R., Elbers, J., Granier, A., Grünwald, T., Morgenstern, K., Pilegaard, K., Rebmann, C., Snijders, W., Valentini, R., Vesala, T., 2000. Estimates of the annual net carbon and water exchange of forests: the EUROFLUX methodology. Adv. Ecol. Res. 30, 113–175.

Aubinet, M., Chermanne, B., Vandenhaute, M., Longdoz, B., Yernaux, M., Laitat, E., 2001. Long-term carbon dioxide exchange above a mixed forest in the Belgian Ardennes. Agric. Forest Meteorol. 108, 293–315.

Dagnelie, P., 1991. Théorie et Méthodes Statistiques. Presses Agronomiques de Gembloux, Gembloux, Belgium, 378 pp.

FAO, 2003. FAO Statistical Databases. Available on: http://faostat.-fao.org/.

Freibauer, A., Rounsevell, M.D.A., Smith, P., Verhagen, J., 2004. Carbon sequestration in the agricultural soils of Europe. Geoderma 122, 1–23.

Grelle, A., Lindroth, A., 1996. Eddy-correlation system for long-term monitoring of fluxes of heat, water vapour and CO_2. Glob. Change Biol. 2 (3), 297–307.

Hanan, N.P., Berry, J.A., Verma, S.B., Walter-Shea, E.A., Suyker, A.E., Burba, G.G., Denning, A.S., 2005. Testing a model of CO_2, water and energy exchange in Great Plains tall grass prairie and wheat ecosystems. Agric. Forest Meteorol. 131, 162–179.

Janssens, I., Dore, S., Epron, D., Lankreijer, H., Buchmann, N., Longdoz, B., Brossaud, J., Montagnani, L., 2003. Climatic influences on seasonal and spatial differences in soil CO_2 efflux. In: Valentini, R. (Ed.), Fluxes of Carbon, Water and Energy of European Forests, Ecological Studies, 163. Springer, Berlin, pp. 233–253.

Leuning, R., 1995. A critical appraisal of a combined stomatal-photosynthesis model for C_3 plants. Plant Cell Environ. 18, 339–355.

Li-Cor Biosciences Inc., 2003. Using the LI-6400 Version 5. Li-Cor Inc., Lincoln, Nebraska, USA.

Lloyd, J., Taylor, J.A., 1994. On the temperature dependence of soil respiration. Funct. Ecol. 8, 315–323.

Moncrieff, J.B., Massheder, J.M., de Bruin, H., Elbers, J., Friborg, T., Heusinkveld, B., Kabat, P., Scott, S., Soegaard, H., Verhoef, A., 1997. A system to measure surface fluxes of momentum, sensible heat, water vapour and carbon dioxide. J. Hydrol. 188–189, 589–611.

Monteith, J.L., Unsworth, M.H., 1990. Principles of Environmental Physics. Edward Arnold, London, England, 291 pp.

Moureaux, C., Debacq, A., Bodson, B., Heinesch, B., Aubinet, M., 2006. Annual net ecosystem carbon exchange by a sugar beet crop. Agric. Forest Meteorol. 139, 25–39.

Moureaux, C., Debacq, A., Hoyaux, J., Suleau, M., Tourneur, D., Bodson B., Aubinet, A., in press. Carbon balance assessment of a Belgian winter wheat crop (*Triticum aestivum* L.).

MRW-DGA, 2005. L'évolution de l'économie agricole et horticole de la Région wallonne 2003. MRW-DGA.

Rodriguez, D., Keltjens, W.G., Goudriaan, J., 1998. Plant leaf area expansion and assimilate production in wheat (*Triticum aestivum* L.) growing under low phosphorus conditions. Plant Soil 200, 227–240.

Rodriguez, D., Ewert, F., Goudriaan, J., Manderscheid, R., Burkart, S., Weigel, H.J., 2000. Modelling the response of wheat canopy assimilation to atmospheric CO_2 concentrations. New Phytol. 150, 337–346.

Ruimy, A., Jarvis, P.G., Baldocchi, D., Saugier, B., 1995. CO_2 fluxes over plant canopies and solar radiation: a review. Adv. Ecol. Res. 26, 1–65.

Schulze, E.-D., Hall, A.E., 1982. Stomatal responses, water loss and CO_2 assimilation rates of plants in contrasting environments. In: Lange, O., Nobel, P.S., Osmond, C.B., Zeigler, H. (Eds.), Encyclopedia of Plant Physiology, 12B. Springer, Berlin, pp. 181–230.

Soegaard, H., Thorgeirsson, H., 1998. Carbon dioxide exchange at leaf and canopy scale for agricultural crops in the boreal environment. J. Hydrol. 212–213, 51–61.

Suyker, A.E., Verma, S.B., Burba, G.G., Arkebauer, T.J., Walters, D.T., Hubbard, K.G., 2004. Growing season carbon dioxide

exchange in irrigated and rainfed maize. Agric. Forest Meteorol. 124, 1–13.
Tewolde, H., Dobrenz, A.K., Voigt, R.L., 1993. Seasonal trends in leaf photosynthesis and stomatal conductance of drought stressed and nonstressed pearl millet as associated to vapour pressure deficit. Photosynth. Res. 38, 41–49.
Van't Hoff, J., 1898. Lectures on Theoretical and Physical Chemistry. Part I. Chemical Dynamics. Edward Arnold, London, England, pp. 224–229.
Veneklaas, E., Van Den Boogaard, R., 1994. Leaf age-structure effects on plant water use and photosynthesis of two wheat cultivars. New Phytol. 128, 331–337.
Xue, Q., Weiss, A., Arkebauer, T.J., Baenziger, P.S., 2004. Influence of soil water status and atmospheric vapour pressure deficit on leaf gas exchange in field-grown winter wheat. Environ. Exp. Bot. 51, 167–179.
Zadoks, J.C., Chang, T.T., Konzak, C.F., 1974. A decimal code for the growth stages of cereals. Weed Res. 14 (6), 415–421.